

Recombination and thermal emission of excitons in shallow CdTe/Cd_{1-x}Mg_xTe quantum wells

R. Spiegel, G. Bacher, K. Herz, and A. Forchel

Technische Physik, Universität Würzburg, Am Hubland, 97074 Würzburg, Germany

T. Litz, A. Waag, and G. Landwehr

Experimentelle Physik III, Universität Würzburg, Am Hubland, 97074 Würzburg, Germany

(Received 16 June 1995)

The recombination dynamics of excitons in shallow CdTe/Cd_{1-x}Mg_xTe multiple single quantum wells has been investigated. In the low-temperature regime ($T \leq 50$ K), radiative recombination dominates the decay of the excitonic luminescence. The low-temperature lifetime as well as the increase of the lifetime with temperature are strongly well-width dependent, due to the correlation between the exciton binding energy and the radiative lifetime. At high temperatures, a decrease of the lifetime and of the photoluminescence intensity is observed that depends on the well width and the Mg content in the barrier. By analyzing transient photoluminescence spectra, carrier capture and thermal emission were studied. Within the first picoseconds after the excitation, the carriers are distributed between the quantum wells by a fast capture process. Subsequently, thermal emission reduces the population in shallow quantum wells inducing a transfer between the quantum wells via barrier states.

I. INTRODUCTION

Excitons in II-IV quantum-well structures have been the subject of many investigations¹⁻⁷ due to their interesting physical properties and the large progress of epitaxial techniques for II-VI heterostructures of high quality. The possibility to tune the band gap over the whole visible range simply by varying the composition of II-VI quantum wells is a promising basis for applications in optoelectronic and electronic devices. A detailed understanding of the recombination dynamics, particularly of the interplay between radiative and nonradiative recombination channels, is therefore of special interest.

In II-VI heterostructures, the exciton oscillator strength is expected to be quite high, resulting, e.g., in enhanced radiative recombination rates compared to GaAs- or InP-based III-V compounds.⁴⁻⁷ In the low-temperature regime a linear increase of the excitonic lifetime with temperature was found in the CdTe/Cd_{1-x}Mn_xTe system, as expected for free excitons, while no dependence of the radiative lifetime on well thickness could be observed.³ At elevated temperatures, nonradiative recombination reduces both the photoluminescence (PL) efficiency and the recombination lifetime.^{3,7} An important nonradiative loss channel expected even in ideal quantum wells is the thermal emission of carriers out of quantum-well states into the barrier. This process, which is mainly important for shallow quantum wells, was discussed in a number of studies for different III-V heterostructures.⁸⁻¹² For II-VI quantum wells, in contrast, there is still little information about the transient capture and emission dynamics.

In this paper we present a study of the exciton dynamics in a set of thin CdTe/Cd_{1-x}Mg_xTe quantum wells with varying well thickness and magnesium content. The CdTe/Cd_{1-x}Mg_xTe material system was selected because it is on one side possible to adjust the energy discontinuity between the barrier and the well material band gap over a large energy range simply by varying the magnesium content

in the barrier.¹³ On the other side, II-VI materials are characterized by larger exciton binding energies compared to III-V quantum-well structures resulting in optical properties determined by excitons even at room temperature.¹⁴ For that reason, we can neglect the thermal dissociation of excitons in the temperature range under consideration ($T < 200$ K). By time-resolved and time-integrated PL measurements we have focused on the temperature dependence of the exciton recombination dynamics, characterized by radiative recombination in the low-temperature range and the thermal emission of carriers into the barriers at high temperatures. Transient PL spectra of especially designed multiple single-quantum-well heterostructures directly reflect the carrier collection and thermally induced transfer processes between the quantum wells via barrier states.

II. EXPERIMENTAL DETAILS

The CdTe/Cd_{1-x}Mg_xTe structures under investigation were grown by molecular-beam epitaxy on a (100)-oriented undoped Cd_{0.96}Zn_{0.04}Te substrate at a growth temperature of 240 °C, as described in detail by Waag *et al.*¹³ Each sample consists of three CdTe quantum wells with nominal widths $L_z = 2.5, 5,$ and 7.5 nm (sample A) and $L_z = 2, 4,$ and 8 nm (sample B) separated by 20- (sample A) and 50-nm-wide (sample B) Cd_{1-x}Mg_xTe barriers, respectively. The magnesium content was determined from the PL signal of the barrier to $x = 0.24$ in sample A and $x = 0.12$ in sample B. Time-resolved PL experiments were performed using a frequency-doubled mode-locked Ti-sapphire laser yielding pulses with a pulse width of 2 ps and a repetition rate of 82 MHz. The laser wavelength was tuned to 405 nm, thus creating carriers above the Cd_{1-x}Mg_xTe band gap. The excitation peak density was about 100 kW/cm². This corresponds to exciton densities in the range of 5×10^{10} cm⁻² per pulse in each quantum well, if we take into account a reflection of about 25% of the incident light at the sample surface and an iden-

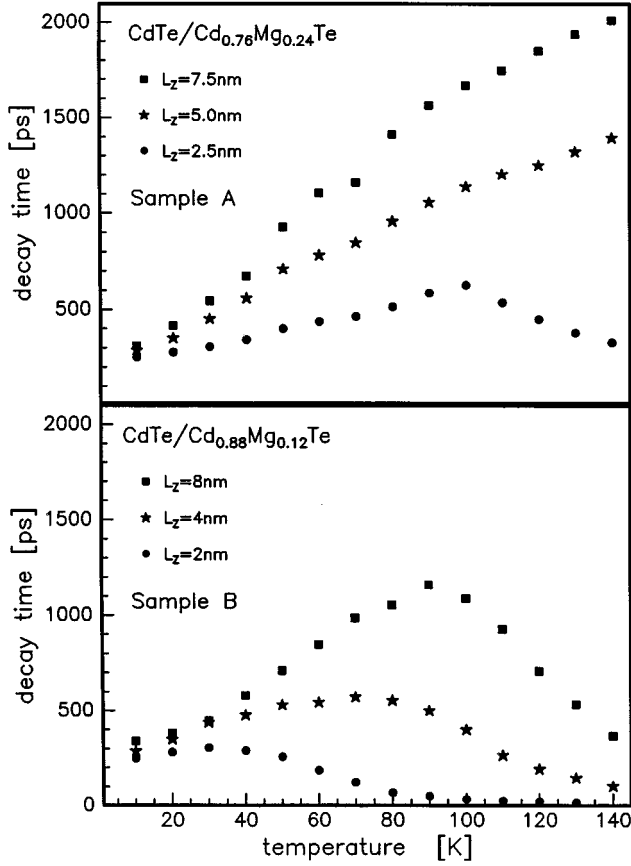


FIG. 1. PL decay times of different quantum wells in samples A (top) and B (bottom) as a function of temperature.

tical sharing of the excess carriers between the three quantum wells and the two loss channels sample surface and substrate. The luminescence signal was dispersed by a 0.32-m spectrometer with spectral resolution better than 0.2 nm and detected by a synchroscan streak camera providing a temporal resolution of less than 10 ps. For comparison, cw measurements have been performed using the 514.5-nm line of an argon ion laser (average excitation density of 5 W/cm²) for the excitation and a charge coupled device camera for the detection.

III. RESULTS AND DISCUSSION

In Fig. 1 a comparison of the PL decay times of sample A and sample B is depicted as a function of temperature for different well widths L_z . While at low temperatures and for low-density cw excitation an additional contribution of a D^0X transition can be observed, free exciton recombination dominates for pulsed excitation. The decay times shown in Fig. 1 were deduced from the monoexponential decay of the free exciton PL signal. First, we discuss the quantum-well width dependence of the exciton lifetime at low temperatures. In both samples a distinct reduction of the decay time for decreasing well width is observed, yielding, e.g., for sample A at $T = 10$ K a lifetime of 320 ps for $L_z = 7.5$ nm and 240 ps for $L_z = 2.5$ nm. Second, we observe a characteristic temperature dependence of the exciton lifetime. Increasing the temperature results in a linear increase of the decay time,

which strongly depends on the well width and Mg content. The slope of the lifetime increase is about 14 ps/K for $L_z = 7.5$ nm and 4 ps/K for $L_z = 2.5$ nm in sample A. Slightly smaller values are found in sample B, which has a lower Mg content in the barrier. It is important to note that at least for $T \leq 50$ K the PL intensity of each quantum well remains fairly constant (see below, Fig. 2). Therefore, we conclude that in this temperature range radiative recombination is the dominating recombination mechanism of the free excitons. The increase of the decay time with temperature thus reflects the temperature dependence of the radiative lifetime. In the high-temperature regime nonradiative carrier loss occurs, decreasing the exciton lifetime. This can be seen clearly in the data of the $L_z = 2.5$ nm quantum well of sample A, as well as for all quantum wells in sample B at $T \geq 80$ K. A comparison of the experimental data of samples A and B shows that the reduction of the decay time depends, on the one hand, on the well width, and, on the other hand, on the Mg content.

For the interpretation of these experimental results, we first have to discuss the correlation between the radiative exciton lifetime τ_s , the exciton binding energy E_B , and the homogeneous linewidth Γ_{hom} as given by Feldmann *et al.*:¹⁵

$$\tau_s \propto \frac{1}{E_B} \cdot \frac{\Gamma_{\text{hom}}}{1 - \exp(-\Gamma_{\text{hom}}/k_B T)}, \quad (1)$$

i.e., the radiative lifetime is proportional to the inverse of the exciton binding energy. The exciton binding energy is expected to be enhanced in narrow quantum wells.¹⁶ In the CdTe/ZnTe system, Liu, Rajakarunayake, and McGill have investigated theoretically the dependence of the exciton binding energy on the quantum-well thickness.¹⁷ For a valence-band offset of 200 meV, they reported exciton binding energies ranging from about 18 meV for a quantum-well width of 8 nm to about 23 meV for a 2-nm-wide quantum well. This well width dependence of the exciton binding energies is consistent with the observed decrease of the low-temperature exciton lifetime with decreasing well width, i.e., from 320 ps for $L_z = 7.5$ nm to 240 ps for $L_z = 2.5$ nm in sample A and from 340 ps for $L_z = 8$ nm to 250 ps for $L_z = 2$ nm in sample B. Although localization effects cannot be fully ruled out, especially in the narrowest quantum wells (see the discussion below), this confirms that the well width dependence of the low-temperature exciton lifetime mainly reflects the correlation between the exciton binding energy and the radiative recombination lifetime. Compared to GaAs/Al_xGa_{1-x}As (Ref. 15) or In_xGa_{1-x}As/InP (Ref. 18) quantum wells, the observed lifetime is much lower, reflecting the enhanced exciton binding energies in II-VI materials. In contrast to former experiments on CdTe/Cd_{1-x}Mn_xTe quantum wells,³ we observe a distinct well width dependence of the low-temperature exciton lifetimes in our CdTe/Cd_{1-x}Mg_xTe structures. However, the increase of the exciton lifetime with well width of 16 ps/nm is considerably lower than, e.g., in GaAs/Al_xGa_{1-x}As quantum wells, where values of 100 ps/nm have been observed.¹⁵

In order to model the linear increase of the lifetime with temperature the magnitude of the homogeneous broadening Γ_{hom} should be known. Degenerate four-wave-mixing experiments have been performed by Hellmann *et al.*¹⁹ on CdTe/Cd_{0.56}Mg_{0.44}Te quantum wells. They reported T_2 val-

ues, corresponding to a homogeneous broadening of $\Gamma_{\text{hom}} = 0.14$ meV at $T = 10$ K, increasing with temperature by $5 \mu\text{eV/K}$. As the barrier Mg content of our samples is even lower, we can assume similar or even lower values of Γ_{hom} and we get $k_B T \gg \Gamma_{\text{hom}}$ in the temperature range where radiative recombination dominates the exciton lifetime ($10 \text{ K} \leq T \leq 50 \text{ K}$). Therefore Eq. (1) approximately reads $\tau_s \propto T/E_B$. This indicates that the observed well-width-dependent increase of the exciton lifetime with temperature mainly reflects the correlation between the radiative lifetime and the exciton binding energy. Being more quantitatively, however, it has to be noted that in the case of the $L_z = 2.5$ nm quantum well of sample A the increase of the lifetime with temperature is quite small when compared to the wider quantum wells. A similar behavior was already observed in GaAs/Al_xGa_{1-x}As quantum wells¹⁵ and related to the influence of exciton localization in narrow quantum wells, causing a smaller slope of τ versus T as simply expected from the correlation between lifetime and exciton binding energy.

As the observed decrease of the lifetime in the high-temperature regime strongly depends on well width and Mg content (see Fig. 1), we conclude that the thermal activation of excitons out of the quantum wells into the barriers is the most significant carrier loss process.^{8,9,12} From the barriers the carriers can be captured by neighboring quantum wells or recombine nonradiatively in the substrate or at the sample surface, thus reducing the lifetime in the quantum well under investigation. The thermal emission process strongly depends on the confinement energy, as defined by the energetic difference between the barrier and the quantum-well emission. The smaller the confinement energy (e.g., smaller well width or lower Mg content in the barrier), the higher the thermal emission rate at a given temperature. This can be seen very easily in sample B (right-hand side of Fig. 1). Because of the lower confinement energy, e.g., in the $L_z = 2$ nm quantum well, the thermal emission reduces the decay time already at temperatures $T > 30$ K, whereas a reduction of the decay time in the $L_z = 8$ nm quantum well is only observed at temperatures above 90 K. Increasing the Mg content in the barrier, the emission rate is reduced, as can easily be seen by a comparison of the narrowest quantum wells in samples A and B.

In order to determine the activation energy, which characterizes the thermal emission process, we have performed time-integrated PL measurements. A set of PL spectra at different temperatures for the sample B is shown in Fig. 2. Besides the dominating PL signal from the quantum wells, also a weak PL signal from the barrier can be observed (not shown in the figure), which vanishes at elevated temperatures due to an enhanced carrier capture into the quantum wells. As already mentioned above, the PL intensity of all quantum wells remains almost constant at low temperatures $T < 50$ K. Increasing the temperature, a well-width-dependent reduction of the PL intensity is observed, first quenching the PL intensity of the smallest quantum well. At temperatures above 130 K the luminescence from the $L_z = 8$ nm quantum well dominates the spectrum.

In the inset of Fig. 2, the integrated PL intensity is depicted versus temperature in an Arrhenius plot for the different quantum wells of sample B. While at low temperatures the PL intensity is almost constant, an increase of the tem-

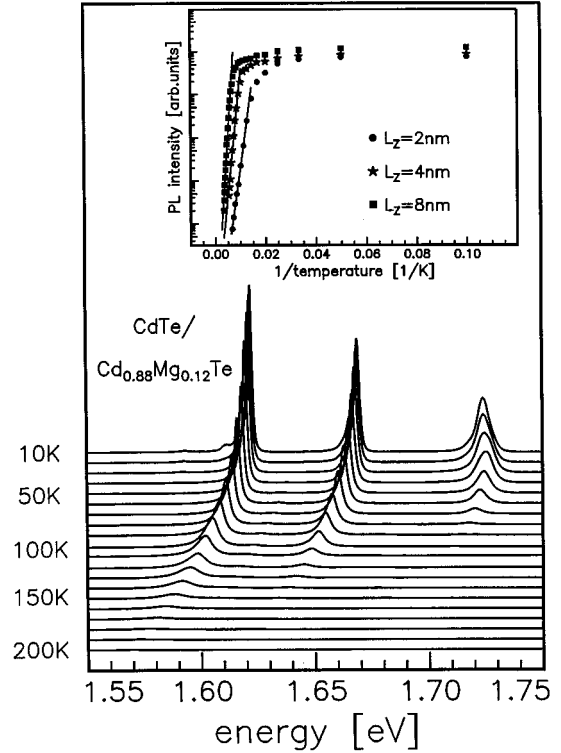


FIG. 2. Time-integrated PL spectra of a CdTe/Cd_{0.88}Mg_{0.12}Te multiple single quantum well (sample B) for different temperatures. In the inset, an Arrhenius plot of the quantum-well intensity is shown for different well widths L_z .

perature results in a distinct drop of the PL intensity. The slope of the decrease is characterized by an activation energy E_A indicated by the linear fit of the data.²⁰ In Table I, the activation energies E_A of the different quantum wells are compared with the corresponding exciton confinement energies E_C as obtained from the difference between the barrier and quantum-well emission energies. Within less than 10%, good agreement between E_A and E_C is found, confirming that indeed the thermal emission of excitons out of quantum-well states into the barriers controls the nonradiative carrier loss at high temperatures.

While cw spectra only yield information about the quasi-equilibrium distribution of the excitons between quantum-well and barrier states, transient spectra reveal the dynamics of the carrier capture and emission process. In Fig. 3 transient PL spectra of sample B measured at a temperature of 120 K are displayed. At this temperature, the exciton dynamics is strongly influenced by the thermal emission process

TABLE I. Comparison of activation energies E_A extracted from Arrhenius plots of the luminescence intensity and exciton confinement energies E_C , as extracted from the PL spectra for the three different quantum wells in sample B.

L_z (nm)	E_A (meV)	E_C (meV)
2	83	78
4	125	135
8	176	177

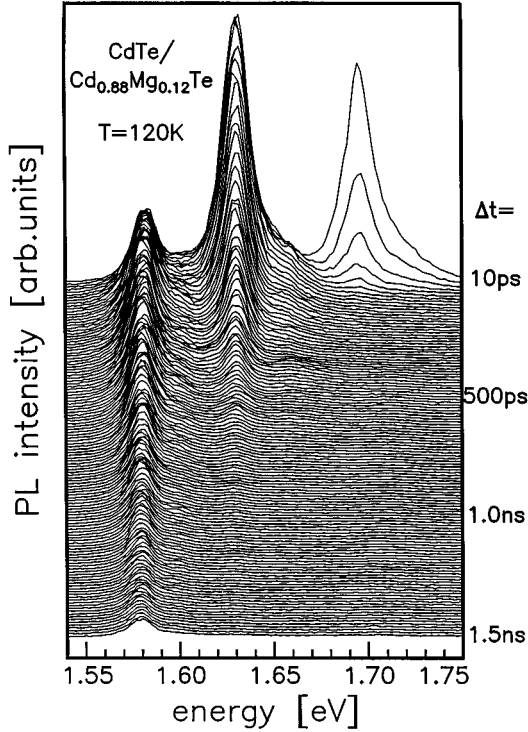


FIG. 3. Transient PL spectra of sample B at $T=120$ K. Δt indicates the delay time after excitation by a short laser pulse.

(see Figs. 1 and 2). For example, in the cw spectrum the PL intensity of the 2-nm quantum well is quenched totally. In the time-resolved spectra shown in Fig. 3, in contrast, a strong emission of this quantum well is observed shortly after the laser pulse ($\Delta t=10$ ps). This indicates an efficient carrier capture into the 2-nm quantum well also at high temperatures.²¹ After about 40 ps thermal reemission of carriers into the barrier decreases the PL intensity of the smallest quantum well drastically. For increasing time, thermal emission also reduces the signal of the 4-nm quantum well and for $\Delta t > 800$ ps the luminescence line of the 8-nm quantum well dominates the spectrum. We want to emphasize that the contribution of the different quantum wells to the PL spectrum shortly after the excitation by a laser pulse ($\Delta t < 40$ ps) is independent of temperature. Only the total number of carriers captured by the quantum wells is reduced at higher temperatures (mainly due to nonradiative losses at the sample surface or in the substrate) causing a decrease of the spectrally integrated PL intensity at elevated temperatures. From these results we conclude that the emission dynamics in the structures investigated can be separated in two steps. First, a fast carrier capture process causes an almost-temperature-independent exciton distribution between the quantum wells, each in thermal equilibrium with the neighboring parts of the barriers. In a second step, thermal emission and recapture in neighboring quantum wells leads to a redistribution of the carriers between the quantum wells, a process becoming more efficient at high temperatures.

This result is summarized in Fig. 4, where the decay curves of the three quantum wells of sample B are displayed at a temperature of 120 K. Different time ranges indicated by

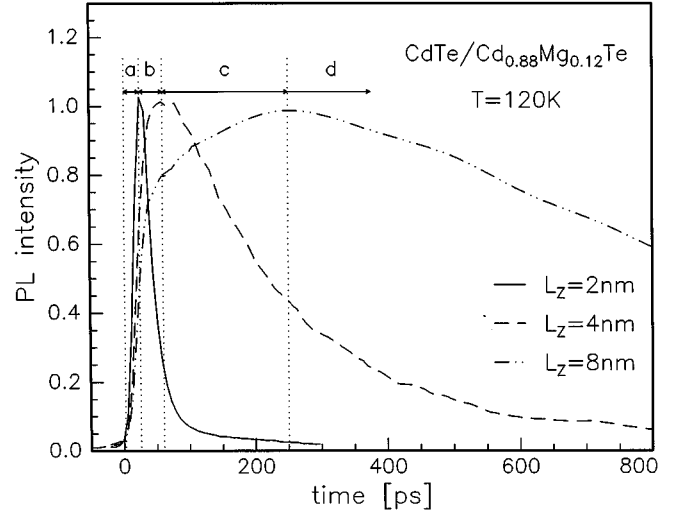


FIG. 4. Normalized PL intensity as a function of time for three quantum wells of sample B at $T=120$ K. The four different time ranges $a-d$ are indicated by the dotted lines and are explained in the text.

the dotted vertical lines can be distinguished. At delay times $\Delta t < 30$ ps, a fast increase of the PL intensity indicates an efficient carrier collection into each quantum well (a). After this time regime thermal emission of carriers starts in the 2-nm quantum well, reducing drastically the PL intensity of the narrowest quantum well (b). Simultaneously, an additional slower component is observed in the onset of the wider quantum wells. For $\Delta t > 60$ ps, an efficient thermally induced transfer of carriers between the 4-nm quantum well and the 8-nm quantum well is observed causing an additional delayed onset of the intensity of the 8-nm quantum well (c). For delay times larger than 250 ps, the PL intensity decreases even for the 8-nm quantum well (d). The correlation between the decay of the PL intensity in the narrower quantum wells and the onset of the wide quantum-well signal clearly demonstrates the transfer between the quantum wells caused by a thermal coupling via barrier states.

IV. CONCLUSION

In summary, we have investigated the exciton dynamics in CdTe/Cd_{1-x}Mg_xTe quantum wells by time-resolved and time-integrated PL spectroscopy. At temperatures below 50 K the exciton decay time is dominated by radiative recombination. The well width dependence of the low-temperature lifetimes reflects the variation of the exciton binding energy. At low temperatures the exciton lifetime increases with a well-width-dependent slope between 15 and 4 ps/K, significantly smaller than, e.g., in GaAs/Al_xGa_{1-x}As quantum wells. This is partially explained by the enhanced exciton binding energies in CdTe/Cd_{1-x}Mg_xTe quantum wells compared to III-V compounds. At high temperatures thermal emission of carriers out of the quantum wells into the barriers reduces the exciton decay time as well as the PL intensity. While the initial capture process causes a carrier distribution between the quantum wells nearly independent of temperature, thermally induced transfer between the quan-

tum wells takes place at elevated temperatures. This process is especially pronounced in shallow quantum wells and therefore expected to reduce the luminescence efficiency also in other II-VI heterostructures, such as $\text{Cd}_x\text{Zn}_{1-x}\text{Se}/\text{ZnSe}$ or $\text{ZnSe}/\text{ZnSe}_{1-x}\text{S}_x$ with small confinement energies.

ACKNOWLEDGMENT

We gratefully acknowledge the financial support of this work by the Deutsche Forschungsgemeinschaft, Grant No. SFB 410.

-
- ¹R. P. Stanley, J. Hegarty, R. Fischer, J. Feldmann, E. O. Göbel, R. D. Feldman, and R. F. Austin, *Phys. Rev. Lett.* **67**, 128 (1991).
- ²J. H. Collet, H. Kalt, L. S. Dang, J. Cibert, K. Seminadayar, and S. Tatarenko, *Phys. Rev. B* **43**, 6843 (1991).
- ³A. Pohlmann, R. Hellmann, E. O. Göbel, D. R. Yakovlev, W. Ossau, A. Waag, R. N. Bicknell-Tassius, and G. Landwehr, *Appl. Phys. Lett.* **61**, 2929 (1992).
- ⁴J. Cui, H. L. Wang, F. X. Gan, X. G. Huang, Z. G. Cai, Q. X. Li, and Z. X. Yu, *Appl. Phys. Lett.* **61**, 1540 (1992).
- ⁵M. O'Neill, M. Oestreich, W. W. Rühle, and D. E. Ashenford, *Phys. Rev. B* **48**, 8980 (1993).
- ⁶T. Stirner, W. E. Hagston, M. O'Neill, and P. Harrison, *J. Vac. Sci. Technol. B* **12**, 1150 (1994).
- ⁷W. Ossau, U. Zehnder, B. Kuhn-Heinrich, A. Waag, T. Litz, G. Landwehr, R. Hellmann, and E. O. Göbel, *Superlatt. Microstruct.* **16**, 5 (1994).
- ⁸G. Bacher, H. Schweizer, J. Kovac, A. Forchel, H. Nickel, W. Schlapp, and R. Lösch, *Phys. Rev. B* **43**, 9312 (1991).
- ⁹P. Michler, A. Hangleiter, M. Moser, M. Geiger, and F. Scholz, *Phys. Rev. B* **46**, 7280 (1992).
- ¹⁰M. Gurioli, J. Martinez-Pastor, M. Colocci, C. Deparis, B. Chastaingt, and J. Massies, *Phys. Rev. B* **46**, 6922 (1992).
- ¹¹J. D. Lambkin, D. J. Dunstan, K. P. Homewood, L. K. Howard, and M. T. Emeny, *Appl. Phys. Lett.* **57**, 1986 (1990).
- ¹²G. Bacher, C. Hartmann, H. Schweizer, T. Held, G. Mahler, and H. Nickel, *Phys. Rev. B* **47**, 9545 (1993).
- ¹³A. Waag, H. Heinke, S. Scholl, C. R. Becker, and G. Landwehr, *J. Cryst. Growth* **131**, 607 (1993).
- ¹⁴N. Pelekanos, J. Ding, A. V. Nurmikko, H. Luo, N. Samarth, and J. K. Furdyna, *Phys. Rev. B* **45**, 6037 (1992).
- ¹⁵J. Feldmann, G. Peter, E. O. Göbel, P. Dawson, K. Moore, C. Foxon, and R. J. Elliot, *Phys. Rev. Lett.* **59**, 2337 (1987).
- ¹⁶B. Kuhn-Heinrich, W. Ossau, H. Heinke, F. Fischer, T. Litz, A. Waag, and G. Landwehr, *Appl. Phys. Lett.* **63**, 2932 (1993).
- ¹⁷Y. X. Liu, Y. Rajakarunanyake, and T. C. McGill, *J. Cryst. Growth* **117**, 742 (1992).
- ¹⁸U. Cebella, G. Bacher, A. Forchel, G. Mayer, and W. T. Tsang, *Phys. Rev. B* **39**, 6257 (1989).
- ¹⁹R. Hellmann, S. T. Cundiff, M. Koch, J. Feldmann, E. O. Göbel, B. Kuhn-Heinrich, D. R. Yakovlev, A. Waag, and G. Landwehr, *Phys. Rev. B* **50**, 14 651 (1994).
- ²⁰As shown by Bacher *et al.* [*Phys. Rev. B* **47**, 9545 (1993)] for $\text{In}_x\text{Ga}_{1-x}\text{As}/\text{GaAs}$ structures, the sample surface in particular, as well as the substrate, can act as efficient nonradiative traps for the carriers in the barrier. The carriers thermally emitted from shallow quantum wells are only partially captured by neighboring wells, while carrier loss occurs in the barrier traps mentioned above. Additionally, in the temperature regime where thermal emission occurs in the narrow wells, a reduction of the PL intensity is observed even in the wider ones (see the inset of Fig. 2). For that reason, no distinct increase of the integrated PL signal in wider wells due to the transfer process can be expected.
- ²¹Note that the percentage of carriers excited directly in the quantum well is only about 4% for the $L_z=2$ nm well and less than 10% for the wider wells. Therefore we have neglected the direct excitation of electron-hole pairs in the wells in the discussion.